Nano Energy (2014) 9, 142–151

Available online at www.sciencedirect.com

ScienceDirect

journal homepage: www.elsevier.com/locate/nanoenergy

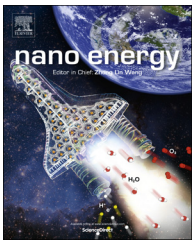

RAPID COMMUNICATION

Remarkable electrochemical stability of one-step synthesized Pd nanoparticles supported on graphene and multi-walled carbon nanotubes

Cauê A. Martins[a,b], Pablo S. Fernández[c], Fabio de Lima[b], Horacio E. Troiani[d], Maria E. Martins[c], Ana Arenillas[e], Gilberto Maia[b], Giuseppe A. Camara[b,*]

[a]*Faculdade de Ciências Exatas e Tecnologia, Universidade Federal da Grande Dourados, 79804-970 Dourados, MS, Brazil*
[b]*Institute of Chemistry, Universidade Federal de Mato Grosso do Sul, C.P. 549, 79070-900 Campo Grande, MS, Brazil*
[c]*Instituto de Investigaciones Fisicoquímicas Teóricas y Aplicadas (INIFTA), Facultad de Ciencias Exactas, UNLP, CCT La Plata-CONICET, C.P. 1900 La Plata, Argentina*
[d]*División Metales, Centro Atómico Bariloche, Av. Ezequiel Bustillo 9500, San Carlos de Bariloche 8400, RN, Argentina*
[e]*Instituto Nacional del Carbón, CSIC, Apartado 73, 33080 Oviedo, Spain*

Received 27 May 2014; received in revised form 7 July 2014; accepted 15 July 2014
Available online 23 July 2014

KEYWORDS
Pd nanoparticles;
Multi-walled carbon nanotubes;
Graphene;
Nanoparticles stability;
Potential cycling

Abstract
Anodes and cathodes of fuel cells are usually composed of metallic nanoparticles (NPs) dispersed on carbon, in order to increase their active area. Since the degradation of the catalyst affects the performance of the fuel cells, understanding the stability of its components is pivotal to make these systems more reliable. As such, graphene sheets and carbon nanotubes have been employed as alternative supports to improve the stability of anodes in fuel cells. In this context, we have used polyvinylpyrrolidone (PVP) combined with a one-step chemical reduction induced by ethylene glycol to synthesize Pd NPs dispersed on chemically converted graphene (CCG). We compared the electrochemical stability of Pd NPs supported on carbon black (C), multi-walled carbon nanotubes (MWCNTs) and CCG. MWCNTs and CCG make Pd NPs electrochemically more stable than carbon black. Pd/CCG catalysts are more stable than Pd/MWCNTs during the first potential cycles, while Pd/MWCNTs showed a higher long-term stability.

*Corresponding author. Tel.: +55 67 3345 3576; fax: +55 67 3345 3552.
E-mail address: giuseppe.silva@ufms.br (G.A. Camara).

http://dx.doi.org/10.1016/j.nanoen.2014.07.009

These results allow us to consider a competition between agglomeration of NPs and degradation of the support, where the agglomeration seems to be limited by the available surface area of the support.

Introduction

Hydrogen-based fuel cells are an alternative to produce energy with low environmental impact. These devices contain metallic nanoparticles (NPs) immobilized on carbon support which are used as cathodes and anodes. However, the electric field experienced by the NPs can provoke a damage in their structure, caused by factors such as (a) metallic dissolution [1], (b) oxidation of NPs with subsequent redeposition upon larger ones (Ostwald ripening) [2], (c) coalescence due to migration and collision of NPs with the surface of support [3,4], (d) detachment of NPs due to carbon corrosion [5] and (e) superficial reorganization of NPs [3]. Further details about the degradation of Pt/C NPs can be found in a review of Meier et al. [6]. Overall, such alterations can induce significant changes in the electrochemical response of a catalyst [3,7,8]. Concerning this subject, collective efforts have been made to synthesize stable Pt [9-11] and Pd NPs [12-14]. For instance, Sasaki et al. reported a new class of stable PdAu catalysts with minimum degradation [15].

Apart from the metallic degradation, the integrity of the carbon support is one of the major factors affecting the lifetime of a fuel cell since it anchors the NPs and works as the electronic collector. Hence, the corrosion of the carbon support greatly contributes to the electrochemical instability of a catalyst [16,17]. In this sense, despite the efforts that supports currently used Pt-based catalysts do not present the durability required for commercial purposes [16], as demonstrated by Mathias et al. for Vulcan carbon® XC-72R supports [18]. Unfortunately, finding substitutes for the commercial carbon black is laborious, mainly because there are few materials containing similar electronic conductivity and equivalent surface areas [19].

In this context, multi-walled carbon nanotubes (MWCNTs) and graphene appear as alternatives for Vulcan carbon® XC-72R in fuel cells applications [19]. Both supports present a well-defined structure containing defects incorporated to the sp2 network, while amorphous carbon exhibits a much higher disorder and massive defective sites [20]. Graphene can be obtained by oxidation of graphite (GR) [21], followed by exfoliation to produce graphene oxide (GO). This carbon-oxide presents characteristics (high surface/volume ratio, high dispersion in aqueous and organic media, and numerous functional groups on the surface) that make it broadly applicable in electrochemistry [22,23]. Furthermore, GO can be easily reduced (as described by Stankovich et al. [24]) to produce chemically converted graphene (CCG).

Graphene sheets decorated with metal nanoparticles are currently attracting special efforts due to their potential for several applications [25]. Different approaches have been used to synthesize dispersed metal NPs on the basal plane of graphene [25], including pre-graphenization, post-graphenization (the reduction of GO is performed after mixing the precursors) and syn-graphenization (one-pot strategy) [26]. There are essentially two ways to prepare metal/graphene nanosheets: (1) simultaneous and (2) sequential reduction of GO and metal precursors [27]. For such, solution-based techniques, where the liquid wets the entire surface of graphene are generally preferred [25]. It has been reported that metallic NPs not only play an essential role in the catalytic reduction of GO, but also prevent its aggregation and restacking (once reduced) by the formation of graphene particle composites [27].

Lei et al. reported high electrochemical performance and stability of a Pt/graphene catalyst assisted with polydiallyldimethylammonium (PDDA) for PEM fuel cells [28]. By using GO as precursor, Xu et al. prepared composites of graphene-metal (Au, Pt and Pd) particles in a water-ethylene glycol mixture and detected typical methanol oxidation profiles during a cyclic voltammetry [29]. Liu et al. used the ethylene glycol reduction method to prepare graphene supported Pt NPs and found that this material presents a better electrocatalytic activity and stability than carbon supported Pt NPs in a borohydride fuel cell operating at 298 K [30]. As an alternative for Pt, Zhang et al. synthesized Pd NPs on graphene sheets by one-pot process and used this material to catalyze the electrooxidation of methanol and ethanol [31]. The authors observed that this material is superior to the commercial Pd-carbon supported catalyst in terms of electrocatalytic activity and electrochemical stability [31].

Regarding studies in alkaline media, Pd catalysts have revealed a remarkable catalysis towards the oxygen reduction reaction (ORR) [32-35]. For instance, Feliu and coauthors have recently investigated the ORR on Pd-nanocubes and found that these materials present an enhanced catalytic activity towards electroreduction of oxygen, which was ascribed to the predominance of the Pd (100) surface sites on the nanocubes [32].

In this sense, new studies addressing the electrochemical stability of supports modified by Pd NPs are still necessary. Here, for the first time, we have used PVP combined with a chemical reduction method induced by ethylene glycol to synthesize Pd NPs dispersed in carbon black, multi-walled carbon nanotubes and chemically converted graphene in order to compare the electrochemical stability of these materials. Another novel aspect of this work is that although a catalyst used in fuel cells might be stable under regular operation, it can rapidly deteriorate under aggressive conditions as start-up and shut-down tests, leading to more severe changes of its morphology. Hence, we emulated these aggressive conditions in electrochemical half-cell experiments, subjecting the catalyst to thousands of successive cyclic voltammograms. Ultimately, this protocol provides reliable information about the performance of a catalyst under controllable experimental conditions.

Experimental

Solutions for synthesis were prepared using ethylene glycol (J.T. Baker), PVP (40,000 g mol^{-1}, Sigma Aldrich), $PdCl_2$ (Sigma Aldrich) and 2-propanol (Vetec).

We prepared Pd NPs supported on Vulcan carbon® XC-72R, MWCNTs and CCG by using ethylene glycol and PVP (EG-PVP) [36] in one-step synthesis [37]. The synthesis of NPs dispersed on Vulcan carbon® XC-72R and MWCNTs was made as described elsewhere [7,38]. Briefly, an aqueous dispersion containing $PdCl_2$, the support and PVP were placed in contact with a solution containing ethylene glycol/water 3:1 (v/v) and heated at 150 °C for 2 h. The molar ratio PVP/metal was set to 0.3 and the amount of palladium was calculated to obtain a metal load of 20% (w/w). Afterwards, this dispersion was washed with water and centrifuged at 4500 rpm for 1 h. This procedure was repeated five times and the remaining dispersion was dried at 60 °C for 24 h. Prior to use, as received MWCNTs (Aldrich, O. D. × I.D. × length 10-20 nm × 5-10 nm × 0.5-200 μm, ≥95%) were cleaned and conditioned for 2 h under reflux at 80 °C in a 5.0 mol L^{-1} HNO_3 solution, thoroughly washed with Milli-Q water and filtered.

GO was synthesized from natural GR powder using the method described by Hummers and Offeman [21] with slight differences, as reported elsewhere [22]. The competition between GO and Pd^{2+} for the reducing agent might limit the amount of metallic nanoparticles and CCG sheets produced. In this sense, we have followed the EG-PVP protocol using 2 and 10 h of reflux, producing NPs hereafter designated as Pd/CCG-2 h and Pd/CCG-10 h, respectively.

The electrochemical stability tests were performed in a three-electrode cell using an oxygen-free 0.1 mol L^{-1} NaOH solution. For the preparation of working electrodes, 32 μL of a 1.0 mg mL^{-1} Pd/support water dispersion were deposited onto a 0.2 cm^2 glassy carbon electrode (polished to a mirror finish) to produce catalysts with a load of 160 μg cm^{-2}. A Pt plate was used as counter electrode. All the potentials were measured against a Ag/AgCl electrode and recalculated to the RHE scale. The catalysts were submitted to 10,000 cycles between −0.7 and 0.45 V vs. Ag/AgCl (0.2-1.35 V vs. RHE). The lower vertex potential was chosen to avoid H_2 adsorption/desorption, which takes place at potentials lower than 0.2 V vs. RHE on Pd [39]. The electrochemically active surface areas (ECSA) were estimated by using the charge involved (420 μC cm^{-2}) in the reduction of a monolayer of PdO [40]. The electrochemical experiments were performed in triplicate.

As synthesized NPs were characterized by scanning electron microscopy (SEM), transmission electron microscopy (TEM) and high resolution TEM (HRTEM), X-ray diffraction (XRD), Raman spectroscopy and N_2 adsorption-desorption isotherms. To evaluate the porosity of the materials, the volumes of the micropores, were determined applying the Dubinin-Radushkevich method (DR) [41]. The specific surface areas were determined by applying the Brunauer-Emmett-Teller (BET) equation to the N_2 adsorption isotherms [42].

SEM images were recorded on a FEI field emission gun (FEG) using a Nova-SEM 230 equipment, working at 5 kV. All samples were assembled on aluminum stubs and coated with gold to ensure good electronic conduction. The chemical composition of the catalysts was determined by using an EDX detector coupled to a SEM JEOL model JSM6380-LV. Two samples of each catalyst were investigated in triplicate. The Raman spectroscopy analyses were carried out in a labRam HRU using JYV-Jobin Yvon equipment and a laser CDPS532-DPSS at 24.3 mW. TEM and HRTEM analyses were recorded in a CM 200 Philips transmission electron microscope, which operates with a LaB_6 emission gun. The microscope is equipped with an ultratwin objective lens and it was operated at 200 keV. The mean diameter of NPs was determined by using the software Axio Vision SE64 Rel.4.8. X-ray diffractograms of the catalysts were recorded in a Siemens model D5000 powder diffractometer, equipped with a monochromatic Cu Kα X-ray source. Diffraction data were collected by step scanning with a step size of 0.02° between 5° and 90°. The porosity of the different supports with Pd NPs was determined by physical adsorption of N_2 at −196 °C, in a Micrometrics ASAP 2010. The samples were degassed at 150 °C under vacuum.

Results and discussion

Chemical composition and crystalline structure of the catalysts

In this section, we describe the structure of Pd/C, Pd/MWCNTs, Pd/CCG-2 h and Pd/CCG-10 h characterized by XRD and Raman spectroscopy. The characterization of GO can be accessed in reference [22].

Table S1 (Supplementary information) shows the chemical composition in terms of mass, determined by six EDX measurements. The carbon mass percentage of all samples is shown in Table S2 (Supplementary information). Pd/C and Pd/MWCNTs NPs present Pd compositions of 6.7% and 8.7%, respectively, while the nominal composition was set to be 20% of Pd (w/w). Pd/CCG-2 h showed a nominal composition of 18.8% of Pd, but even in this case a standard deviation (SD) of ±9.4% was observed for six independent measurements (Table S2). Some factors might contribute to the differences observed between nominal and real compositions. Namely, the time of synthesis was not long enough for a complete Pd deposition on the support surface and the unsupported Pd NPs might be randomly lost during washing and centrifuging procedures. This result indicates a heterogeneous deposition of Pd throughout the surface, which affects the electrochemical measurements (this issue will be further discussed). On the other hand, the real composition of Pd/CCG-10 h was much closer to the nominal one (~20% of Pd) with a lower SD, which reinforces the idea that long times of synthesis are required for a full deposition of Pd NPs onto the support.

The crystalline characterization of the Pd catalysts determined by XRD is shown in Figure 1. The diffraction peak at around $2\theta = 25°$ can be indexed to the (002) plane of carbon [43]. All the other peaks can be assigned to Pd planes [44], and the corresponding XRD patterns are coherent to previous studies [45]. The (111) peak of Pd was used to calculate the average crystallite sizes according to the Scherrer formula [46]

$$t = \frac{0.9\,\lambda}{\beta\,\cos\,\theta} \quad (1)$$

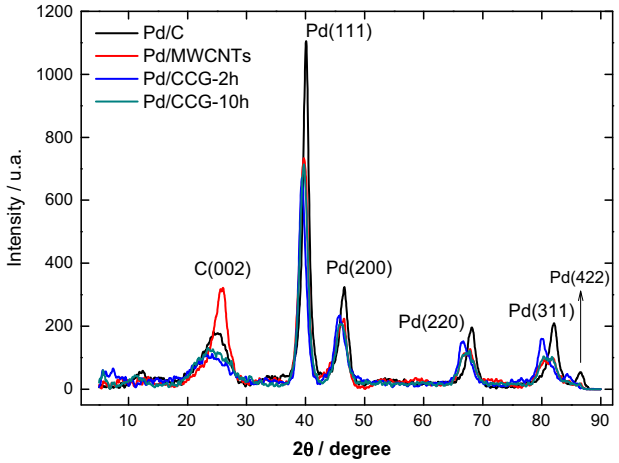

Figure 1 XRD patterns of Pd nanoparticles dispersed over carbon (black curve), multi-walled carbon nanotubes (red curve) and chemically converted graphene for 2 h (blue curve) and 10 h (green curve).

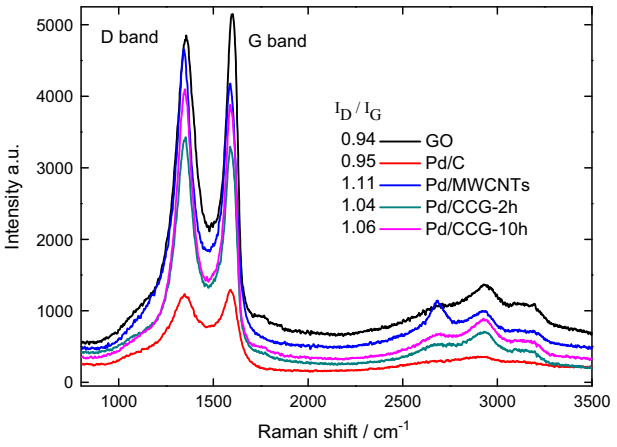

Figure 2 Raman spectra of GO (black curve) and Pd nanoparticles dispersed over carbon (red curve), multi-walled carbon nanotubes (blue curve), chemically converted graphene-2 h (green curve) and 10 h (magenta curve) between 800 and 3500 cm^{-1}.

where t is the crystallite size; 0.9 is an approximated constant for sphere samples; β represents the half-width of the diffraction peak; λ represents the wavelength of the X-ray and θ represents the diffraction angle. The values found were 6.7 nm (for Pd/C), 6.1 nm (Pd/CCG-2 h), 5.3 nm (Pd/CCG-10 h) and 5.1 nm (Pd/MWCNTs).

Furthermore, Figure 1 shows that peaks corresponding to Pd (111), (200), (220) and (311) planes are slightly dislocated to lower degrees for Pd/MWCNT and Pd/CCG compared to Pd/C. Such shifts in the position of the diffraction peaks are feasible for samples with different degrees of crystallinity in different supports and a value of 39.1° for Pd (111) plane is reported for Pd/graphene [47]. Therefore, assuming that each support is different in structure and composition, the displacement of the diffraction peaks is probably caused by the different interaction of the Pd particles with these structures.

The degree of disorder of the carbon structure was investigated by Raman spectroscopy. The spectra were collected between 800 and 3500 cm^{-1} (Figure 2). A typical graphene monolayer spectrum would present an intense band at ~1582 cm^{-1}, the G band, and a second-order spectrum dominated by a shoulder at ~2717 cm^{-1}, named 2D band [48], which is the overtone (second harmonic) of the D band [49,50]. The D band, at ~1340 cm^{-1}, is absent in defect-free graphite structures and its relative intensity increases with graphitic disorder [49,50].

According to Figure 2, all catalysts present D and G bands at ~1340 and 1595 cm^{-1}, respectively, indicating a certain degree of disorder. However, all materials except for Pd/C, present the second order spectra with well-defined peaks between 2500 and 3500 cm^{-1}, indicating that they have some three-dimensional order. It is worth to mention that these second order spectra are qualitatively similar to GO, Pd/CCG-2 h and Pd/CCG-10 h, indicating similar structures. On the other hand, the spectrum of Pd/MWCNTs is quite different and indicates a different three-dimensional structure. At this point, it is important noting that regarding their disorder degree, is difficult to quantitatively compare the samples, because they present heteroatoms in their structure (GO has oxygen while Pd is present in all other samples). Usually, the intensity ratio of the D and G bands (I_D/I_G) is considered to evaluate the extent of order/disorder, as shows the inset in Figure 2. This ratio is expected to increase with the degree of disorder in graphitic materials [49,50]. Figure 2 shows that although similar, the I_D/I_G values show a slight increase of the disorder as GO is reduced to CCG, which agrees with the literature [22,50].

Microscopic characterization of the catalysts

SEM images show that the surfaces of GO, Pd/CCG-2 h and Pd/CCG-10 h are similar (Supplementary Figure S3A, B, C respectively). Both GO and CCG reveal a smooth surface containing hills. Furthermore, CCG shows thin lamellar aggregates, in agreement with the literature [22,24,51-54]. Supplementary Figure S3D and E show Pd NPs immobilized on carbon and MWCNTs, respectively.

The deposition of Pd NP on CCG surface creates superficial defects on the smooth CCG sheet (Supplementary Figure S3B and C), which act as Nucleation Centers for Clustering (NCC). Therefore, Pd NPs might migrate over the support, coalescing in the vicinity of the NCC and generating aggregates. The intrinsic structure of carbon and MWCNTs supports (Supplementary Figure S3D and E respectively) contains higher number of NCC than the smooth CCG support. Hence, the virtually homogeneous distribution of NCC promotes a better distribution of Pd NPs over carbon and MWCNTs, in contrast to CCG.

The porosity of the catalysts was evaluated by N_2 adsorption-desorption isotherms at 196 °C (See Supplementary Figure S4). There is no detectable N_2 adsorption on GO, indicating the absence of available pores. The availability of pores increases as GO is reduced and is very sensitive to the deposition of Pd NPs, as demonstrated by the N_2 adsorption, which follows the sequence GO < Pd/CCG-2 h < Pd/CCG-10 h. The pores with diameters ranging 2-50 nm (mesopores) are especially available, as demonstrated by the higher values of the isotherm at high relative pressures. Pd/C and Pd/MWCNTs

present remarkably higher N_2 adsorption in the whole range of relative pressures.

All materials present low volume of pores, but their total volume ($V_T = V_{micro} + V_{meso}$) increases in the following order: GO < Pd/CCG-2 h < Pd/CCG-10 h < Pd/C < Pd/MWCNTs, as can be seen in Table 1. Pd/CCG-2 h < Pd/CCG-10 h merely because longer times of synthesis produce more graphene (in its reduced form). Pd/MWCNTs and Pd/C are mainly mesoporous, with V_{meso} at around 0.3–0.4 cm^3/g. In this context, the helium density (ρ) can be used to estimate the volume of pores (Table 1). Here, it is important to notice that Pd NPs are not expected to present any detectable porosity and then the porosity of each catalyst is mostly determined by the support. Accordingly, high concentrations of Pd in the catalyst do not imply high helium densities.

The morphology and distribution of NPs were investigated by TEM (Figure 3A–D) and HRTEM (Figure 3E–L). Pd NPs are well dispersed on carbon and mostly spherical (Figure 3A and I), although some agglomeration can be noticed (Figures 3A and 5E). On the other hand, TEM and HRTEM images of Pd/MWCNTs (Figure 3B, F and J, respectively) show nanotubes absent of Pd and regions containing aggregates. Figure 3F shows a helical Pd structure over the nanotubes. This characteristic Pd deposition on carbon nanotubes was previously reported by Cai et al., by using hexadecyltrimethylammonium bromide in the synthesis [55] and reinforces that the deposition of Pd is sensitive to the morphology of the support. The comparison of Figure 3C–G with Figure 3D–H (CCG modified Pd NPs after 2 and 10 h of synthesis and their corresponding high resolution images) makes clear that the agglomeration effect during the synthesis seems to be more intense on CCG. This result corroborates the hypothesis of a stronger agglomeration over smoother supports.

Although the presence of aggregates and the heterogeneity of the NPs hinder the identification of individual particles by TEM, we estimated the average size after counting 300 NPs of each catalyst, as show the histograms in Figure 3A–D. Considering the standard deviation (SD), the catalysts presented similar average sizes. In general, these values are consistent with the average crystallite size calculated by XRD, and the minor differences seem to be not significant for the present analysis.

Evaluation of the electrochemical stability of Pd NPs dispersed over different supports

Studies of catalysts for fuel cell typically involve the monitoring of their electrochemical stability [3,6,10,36,56,57]. Although a catalyst used in fuel cells might be stable under regular operation, it can rapidly deteriorate under aggressive conditions as start-up and shut-down tests, leading to more severe losses of its surface area [58]. These aggressive conditions can sometimes be simulated in electrochemical half-cell experiments, subjecting the catalyst to successive cyclic voltammograms [6]. Although this protocol cannot reproduce all the phenomena taking place into a fuel cell [59], it provides reliable information about the performance of a catalyst under controllable experimental conditions [6]. Usually, the stability of a catalyst is evaluated by monitoring its electrochemically active surface area during an electrochemical protocol, which involves cyclic voltammetry [3,6,10,36,56,57].

In order to evaluate the stability of one-step synthesized Pd NPs we submit these materials to 10,000 cycles of potential at a high scan rate (1.0 $V\,s^{-1}$) and compare their performances with a homemade Pd/C catalyst (Carbon black was chosen since it is the most spread in the literature and because it is used in fuel cells technology). The broad potential range and the high scan rate were purposely chosen because they simulate extremely aggressive conditions. Figure 4 shows representative voltammograms of the catalysts. The PdO reduction peak (during negative potential going scan) occurs at ~0.5 V for all catalysts. Pd/C shows more defined peaks than the others catalysts (Figure 4A) while Pd/CCG-10 h presents the most prominent peaks for the formation/reduction of PdO among all catalysts. This evidence is in line with the work of Hsieh et al., who have found that Pt/G NPs synthetized at 150 °C for 12 h present high electrochemically active surface areas [37].

The PdO reduction peak on MWCNTs is initially broad and becomes progressively sharper while shifts towards more positive potentials during the potential cycling (Figure 4B). A similar behavior can be seen for Pd/C and Pd/CCG-10 h, Figure 4A and D, respectively. The displacement of the peak cannot be fully understood due to the superimposition of a myriad of effects which contribute for degradation of the catalyst, as aforementioned, but based on numerous literature data, one of the reasons for this observation might be a change of Pd particle size. Moreover, the currents corresponding to the double layer region are sensibly higher for MWCNTs [60] and CCG compared to Pd/C, which merely illustrates the relative high capacitance of these supports [22,31,37]. These massive capacitive currents combined with a possible electron transfer from carboxylic groups probably contribute to a distortion of the electrochemical profiles presented in Figure 4C and D. Moreover, we cannot ignore the possible encapsulation of Pd NPs by graphene sheets, which accounts for increase in the capacitance of the material. Overall, the electrochemical profiles of Pd/CCG-2 h and Pd/CCG-10 h are coherent with those results observed for similar systems [22,31,37].

Table 1 Texture parameters of GO and Pd/C, Pd/MWCNTs, Pd/CCG-2 h and Pd/CCG-10 h NPs obtained by BET isotherms.

Catalysts	S_{BET} (m^2/g)	V_{micro} (cm^3/g)	V_{meso} (cm^3/g)	V_T (cm^3/g)	ρ (g/cm^3)
Pd/C	90	0.034	0.32	0.35	2.284
Pd/MWCNTs	99	0.036	0.43	0.47	2.523
GO	-	-	-	-	1.619
Pd/CCG-2 h	9	0.004	0.05	0.05	1.661
Pd/CCG-10 h	32	0.012	0.13	0.14	1.856

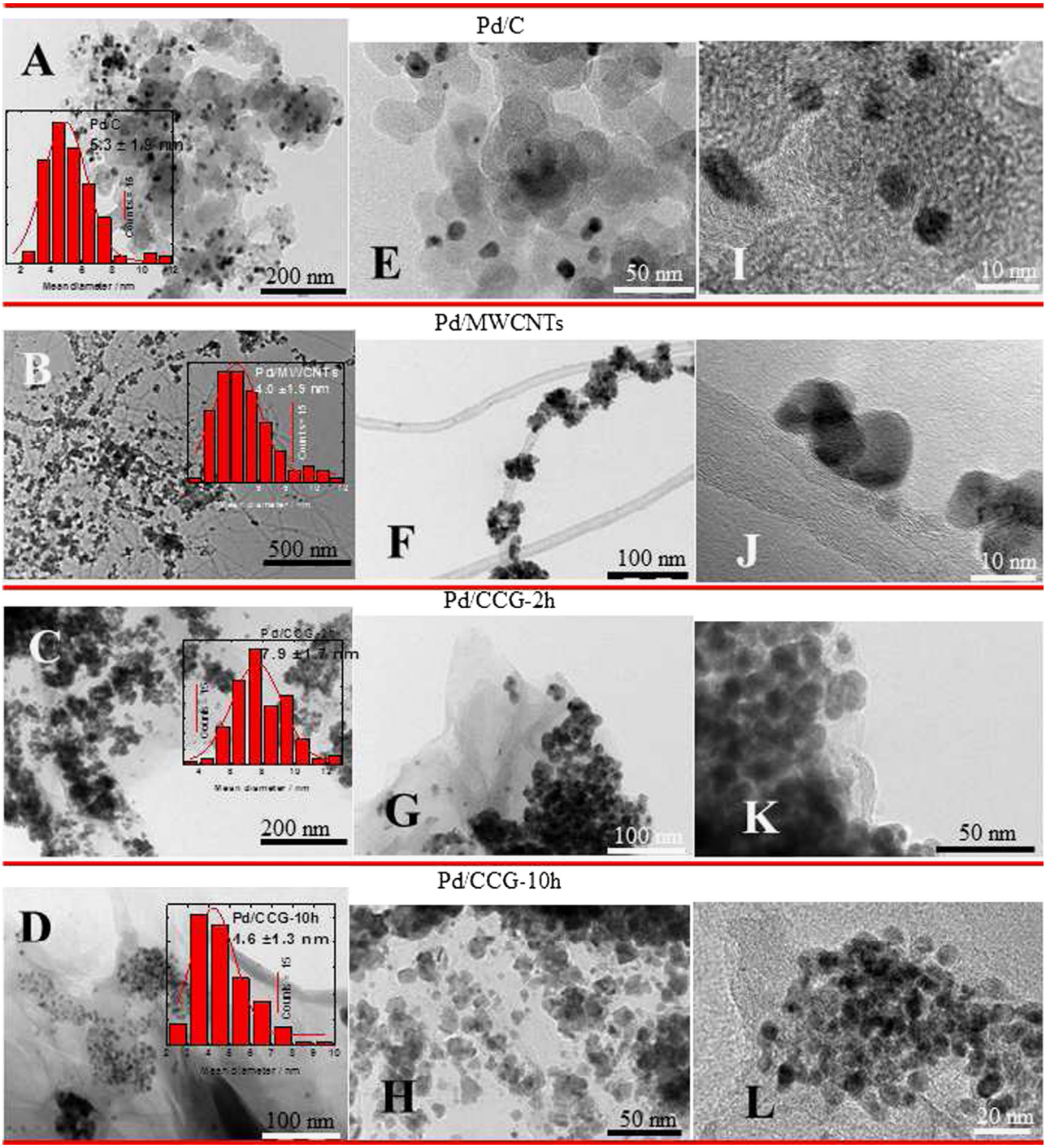

Figure 3 TEM, HRTEM micrographs and average size histograms distribution of (A) Pd/C, (B) Pd/MWCNTs, (C) Pd/CCG-2 h and Pd/CCG-10 h.

The normalized electrochemical active surface areas (calculated from the charge involved in the reduction of a PdO monolayer and normalized by the initial area) are shown in Figure 5 as a function of the number of voltammetric cycles imposed to the catalysts. The first experimental evidence is the low reproducibility of the Pd/CCG-2 h catalysts, especially during the first cycles (inset in Figure 5). Considering that all NPs have the same residues of synthesis on surface, the low reproducibility of Pd/CCG-2 h can be assigned to its heterogeneity, as identified by EDX analysis.

The averages of the initial real non-normalized ECSA for Pd/C, Pd/MWCNTs, Pd/CCG-2 h and Pd/CCG-10 h were 0.94, 1.45, 0.45 and 0.48 cm^2, respectively. The initial ECSA values suggest that the superficial defects of carbon black and nanotubes lead to a higher deposition of Pd compared to graphene. Moreover, a concurrent possibility could be the encapsulation of Pd NPs during the synthesis, which might

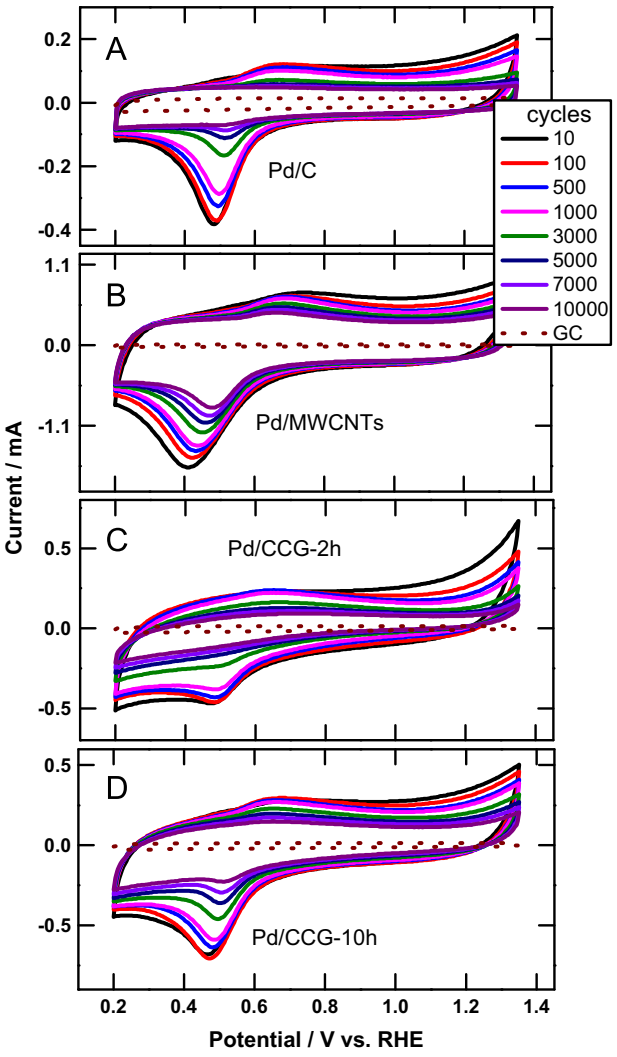

Figure 4 Tests of electrochemical stability: representative voltammograms of 10,000 potential cycling between 0.2 and 1.35 V vs. RHE of (A) Pd/C, (B) Pd/MWCNTs, (C) Pd/CCG-2 h, (D) Pd/CCG-10 h NPs and the glassy carbon (GC) blank in 0.1 mol L^{-1} NaOH at 1.0 V s^{-1}.

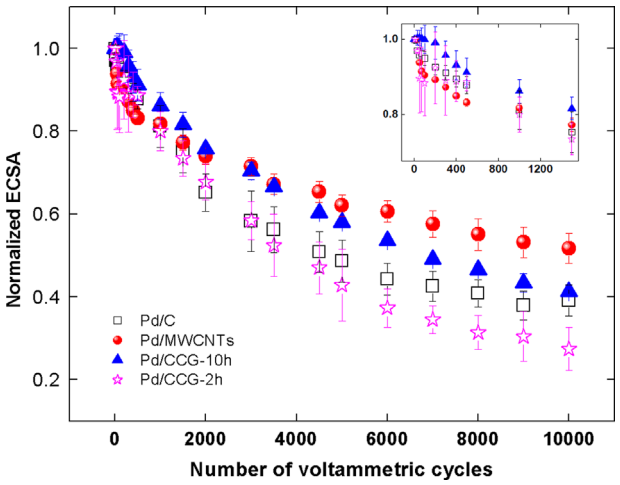

Figure 5 Electrochemically active surface area normalized to the initial surface area as a function of the number of potential cycles. Surface areas obtained from voltammograms performed in 0.1 mol L^{-1} NaOH at 1.0 V s^{-1} for Pd/C, Pd/MWCNTs, Pd/CCG-2 h and Pd/CCG-10 h (indicated in the figure).

reduce the metal load on the surface of the support. Due to the different initial ECSA values for each catalyst the normalization of the initial area seems to be a reasonable way of comparing different materials. This approach will be resumed in further details later.

The ECSA decreases monotonously with the number of cycles for all catalysts. This loss of ECSA can be understood in terms of the degradation phenomena already mentioned, but some works explain the order of the events [3,6,61]. Shao-Horn et al. suggested that the initial degradation could be rationalized as the loss of the smallest NPs due to a rapid dissolution [61]. Additionally, the agglomeration of particles close to each other can also provoke an early degradation [3,6]. In a later event, when NPs became larger, other mechanisms, such as the detachment of NPs due to the degradation of the support, become more relevant than aggregation [6]. Most of the degradation effects were visualized by following an specific location of the sample by microscopic methods as the catalysts were aged [4,5,62]. Now, let us interpret our results in the light of these findings.

The loss of ECSA follows the order Pd/CCG-2 h > Pd/C > Pd/CCG-10 h > Pd/MWCNTs. The worst performance was observed for Pd/CCG-2 h, which loses 73% of the initial area in addition to the low reproducibility. Pd/C quickly loses 62% of the original area. The Pd/C normalized ECSA decreases faster than Pd/CCG-10 h and Pd/MWCNTs before reaching 2000 cycles. The loss of Pd/C ECSA is similar to that observed for Pt/Vulcan by Meier et al. [6]. These authors reported the rapid decrease of ECSA during a degradation test, with a loss of about 61% of the original ECSA after performing 10,800 voltammetric cycles in acid media [6].

Pd/MWCNTs and Pd/CCG-10 h presented the lowest loss of original ECSA, ~48% and 58%, respectively. Although the total ECSA loss for Pd/CCG-10 h is close to that found for Pd/C (62%), the ECSA of Pd/CCG-10 h decreases at a slower rate than Pd/C (Figure 5). These findings evidence that Pd/MWCNTs and one-step synthesized Pd/CCG-10 h (by EG-PVP) improve the electrochemical stability of Pd NPs compared to carbon support in alkaline medium. As demonstrated by BET, Pd/C NPs present higher surface area than Pd/CCG-10 h, but it is not stable, which proves that an initial high surface area is not the only parameter that must be accounted for the choice of a support in catalysis.

Pd/MWCNTs and Pd/CCG-10 h exhibit the best electrochemical stability among the catalysts investigated. During the first 500 cycles, Pd/MWCNTs loses ECSA at a higher rate than Pd/CCG-10 h. We ascribed this initial ECSA decrease to the agglomeration of Pd NPs over the support, causing the increase in the particle size [3]. Afterwards, between ~2000 and ~3500 cycles, the rate of decrease in the area diminishes for Pd/MWCNTs, suggesting that the agglomeration is reaching a limit, while the decay of ECSA of Pd/CCG-10 h remains at a similar rate. After 3500 cycles, the loss of ECSA for Pd/MWCNTs becomes less intense than for Pd/CCG-10 h.

For Pd/CCG-10 h NPs the loss of ECSA can be rationalized as follows: Initially (1st to 2000th cycle), the Pd NPs are well

dispersed on MWCNTs and more aggregated on CCG (Figure 3B-D). In this sense, Pd/MWCNTs contain more Nucleation Centers for Clustering (NCCs) than Pd/CCG. Therefore, during the first cycles, the agglomeration is more intense on the NCCs of MWCNTs than on CCG. Between the 2000th and 3500th cycles, the amount of NCCs on nanotubes diminishes due to the agglomeration, whilst Pd NPs keep agglomerating over CCG. At this stage, it seems that the agglomeration on nanotubes approaches to a limit, restricted by the available surface, while CCG still contains an extensive surface available for coalescence of NPs. After 3500 cycles, the degradation of the Pd/MWCNTs support seems to determine the decrease of the area, while the agglomeration becomes less important (NCCs diminish). At the same stage, Pd NPs behave differently, they keep agglomerating on CCG, and this effect, combined with degradation of the support, contributes to the Pd/CCG-10 h ECSA decay.

In this sense, the availability of a support whose surface is free of NPs seems to play an important role on the agglomeration of NPs themselves, and consequently influences the electrochemical stability of the whole catalyst in a fuel cell. Although the CCG supported catalyst presents high initial stability, its smooth surface compromises its long-term performance when compared to MWCNTs supported catalysts. Our results show that Pd NPs can be easily synthesized over CCG by one-step EG-PVP method, producing catalysts electrochemically more stable than Pd/C in alkaline media. Therefore, CCG and MWCNTs can be considered as promising alternatives to carbon black as a supports for catalysts used in fuel cells.

Conclusion

- The ethylene glycol reduction method with polyvinylpyrrolidone can be used to produce Pd NPs over chemically converted graphene (CCG) in one-step synthesis.
- The graphene oxide and the metal precursor compete for the reducing agent during the synthesis. Hence, long times of synthesis (10 h) are required to produce Pd NPs with homogeneous metal load (w/w).
- The random deposition of Pd on CCG supports during the synthesis can generate Pd domains isolated by graphene sheets, which increase the capacitance of the catalyst, distorting the Pd electrochemical profile.
- Pd NPs dispersed on multi-walled carbon nanotubes (MWCNTs) and on reduced CCG are far more electrochemically stable in alkaline media than Pd dispersed on Vulcan carbon support. These findings make CCG and MWCNTs promising materials for Pd-based catalysts in fuel cells;
- Pd/CCG-10 h is electrochemically more stable during the first 2000 potential cycles, while Pd/MWCNTs showed a higher long-term stability (after 3500 cycles). Between 2000 and 3500 cycles, both catalysts showed similar performance. This discrepancy can be rationalized in terms of a competition between the availability of a support whose surface is free for the agglomeration of nanoparticles and the degradation of the support itself;
- Considering that the development of new stable catalysts for fuel cells is a "hot topic" in energy conversion, our results concerning Pd/CCG and Pd/MWCNTs are relevant since they provide new information about the role of the physical structure of the supports on the electrochemical stability of Pd nanoparticles, which ultimately can help to manufacture stable catalysts aiming their use in alkaline fuel cells.

Acknowledgments

The authors acknowledge financial assistance from CONICET, UNLP, CNPq (Grant # 554591/2010-3), FUNDECT (Grants # 23/200.065/2008 and # 23/200.583/2012), CAPES (No. 05/2013-PNPD 2013), MINCyT and FINEP. P.S. Fernández thanks Consejo Nacional de Investigaciones Científicas y Técnicas (CONICET) for a fellowship. C.A. Martins thanks CNPq (Grant # 140426/2011-6) and CAPES for fellowships (Programa Nacional de Pós-Doutorado # 05/2013-PNPD 2013). Authors want to thank Alejandra Floridia for taking HR-TEM images.

Appendix A. Supporting information

Supplementary data associated with this article can be found in the online version at http://dx.doi.org/10.1016/j.nanoen.2014.07.009.

References

[1] L. Tang, B. Han, K. Persson, C. Friesen, T. He, K. Sieradzki, G. Ceder, J. Am. Chem. Soc. 132 (2010) 596-600.
[2] P.L. Redmond, A.J. Hallock, L.E. Brus, Nano Lett. 5 (2005) 131-135.
[3] C.A. Martins, P.S. Fernández, H.E. Troiani, M.E. Martins, A. Arenillas, G.A. Camara, Electrocatalysis 5 (2014) 204-212.
[4] F.R. Nikkuni, E.A. Ticianelli, L. Dubau, M. Chatenet, Electrocatalysis 4 (2013) 104-116.
[5] K.J.J. Mayrhofer, J.C. Meier, S.J. Ashton, G.K.H. Wiberg, F. Kraus, M. Hanzlik, M. Arenz, Electrochem. Commun. 10 (2008) 1144-1147.
[6] J.C. Meier, C. Galeano, I. Katsounaros, J. Witte, H.J. Bongard, A.A. Topalov, C. Baldizzone, S. Mezzavilla, F. Schüth K.J.J. Mayrhofer, Beilstein J. Nanotechnol. 5 (2014) 44-67.
[7] P.S. Fernández, D.S. Ferreira, C.A. Martins, H.E. Troiani G.A. Camara, M.E. Martins, Electrochim. Acta 98 (2013) 25-31.
[8] C. Grolleau, C. Coutanceau, F. Pierre, J.-M. Léger, Electrochim. Acta 53 (2008) 7157-7165.
[9] H. Lv, S. Mu, N. Cheng, M. Pan, Appl. Catal. B - Environ. 100 (2010) 190-196.
[10] A. Marcu, G. Toth, R. Srivastava, P. Strasser, J. Power Sources 208 (2012) 288-295.
[11] K. Tiido, N. Alexeyeva, M. Couillard, C. Bock, B.R. MacDougall, K. Tammeveski, Electrochim. Acta 107 (2013) 509-517.
[12] J.Y. Wang, H.-X. Zhang, K. Jiang, W.-B. Cai, J. Am. Chem. Soc. 133 (2011) 14876-14879.
[13] T. Harada, S. Ikeda, F. Hashimoto, T. Sakata, K. Ikeue, T. TorimotoM. Matsumura, Langmuir 26 (2010) 17720-17725.
[14] S. Jones, J. Qu, K. Tedsree, X.-Q. Gong, S.C. Edman Tsang, Angew. Chem. 51 (2012) 11275-11278.
[15] K. Sasaki, H. Naohara, Y.M. Choi, Y. Cai, W.-F. Chen, P. Liu R.R. Adzic, Nat. Commun. 3 (2012) 1-9.
[16] Y.-J. Wang, D.P. Wilkinson, J. Zhang, Chem. Rev. 111 (2011) 7625-7651.
[17] J. Ma, A. Habrioux, N. Alonso-Vante, ChemElectroChem 1 (2014) 37-46.

[18] M. Mathias, R. Makharia, H. Gasteiger, J. Conley, T. Fuller, C. Gittleman, S. Kocha, D. Miller, C. Mittesteadt, T. Xie, S. Yan, P. Yu, Electrochem. Soc. Interface 14 (2005) 24–35.
[19] R.V. Noorden, Nature 469 (2011) 14–16.
[20] D.S. Su, S. Perathoner, G. Centi, Chem. Rev. 113 (2013) 5782–5816.
[21] W.S. Hummers Jr., R.E. Offeman, J. Am. Chem. Soc. 80 (1958) 1339.
[22] F. Lima, G.V. Fortunato, G. Maia, RSC Adv. 3 (2013) 9550–9560.
[23] I. Kruusenberg, J. Mondal, L. Matisen, V. Sammelselg, K. Tammeveski, Electrochem. Commun. 33 (2013) 18–22.
[24] S. Stankovich, D.A. Dikin, R.D. Piner, K.A. Kohlhaas, A. Kleinhammes, Y. Jia, Y. Wu, S.T. Nguyen, R.S. Ruoff, Carbon 45 (2007) 1558–1565.
[25] B.F. Machado, P. Serp, Catal. Sci. Technol. 2 (2012) 54–75.
[26] V. Singh, D. Houng, L. Zhai, S. Das, S.I. Khondaker, S. Seal, Prog. Mater. Sci. 56 (2010) 1178–1271.
[27] E. Antolini, Appl. Catal. B – Environ. 123–124 (2012) 52–68.
[28] M. Lei, C. Liang, Y.J. Wang, K. Huang, C.X. Ye, G. Liu, W.J. Wang, S.F. Jin, R. Zhang, D.Y. Fan, H.J. Yang, Y.G. Wang, Electrochim. Acta 113 (2013) 366–372.
[29] C. Xu, X. Wang, J. Zhu, J. Phys. Chem. C 112 (2008) 1984119845.
[30] X. Liu, L. Yi, X. Wang, J. Su, Y. Song, J. Liu, Int. J. Hydrog. Energy 37 (2012) 17984–17991.
[31] Y. Zhang, H. Shu, G. Chang, K. Ji, M. Oyama, X. Liu, Y. He, Electrochim. Acta 109 (2013) 570–576.
[32] H. Erikson, A. Sarapuu, N. Alexeyeva, K. Tammeveski, J. Solla-Gullón, J.M. Feliu, Electrochim. Acta 59 (2012) 329–335.
[33] K. Jukk, N. Alexeyeva, C. Johans, K. Kontturi, K. Tammeveski, J. Electroanal. Chem. 666 (2012) 67–75.
[34] K. Jukk, N. Alexeyeva, P. Ritslaid, J. Kozlova, V. Sammelselg, K. Tammeveski, Electrocatalysis 4 (2013) 42–48.
[35] K. Jukk, N. Alexeyeva, A. Sarapuu, P. Ritslaid, J. Kozlova, V. Sammelselg, K. Tammeveski, Int. J. Hydrog. Energy 38 (2013) 3614–3620.
[36] M. Chen, Y. Xing, Langmuir 21 (2005) 9334–9338.
[37] S.H. Hsieh, M.C. Hsu, W.L. Liu, W.J. Chen, Appl. Surf. Sci. 277 (2013) 223–230.
[38] P.S. Fernández, M.E. Martins, G.A. Camara, Electrochim. Acta 66 (2012) 180–187.
[39] A.E. Bolzán, J. Electroanal. Chem. 380 (1995) 127–138.
[40] H.A. Kozlowska, Comprehensive Treatise of Electrochemistry, in: E.B. Yeager, J.O.M. Bockris, B.E. Conway, S. Sarangapani (Eds.), Plenum Press, New York, 1984, p. 24.
[41] M.M. Dubinin, Progress in surface and Membrane Science, in: D.A. Cadenhead, J.F. Danielli, M.D. Rosenberg (Eds.), Academic Press, New York, 1975, pp. 1–70.
[42] J.B. Parra, J.C. de Sousa, R.C. Bansal, J.J. Pis, J.A. Pajares, Adsorpt. Sci. Technol. 12 (1995) 51–66.
[43] D.M. Gattia, M.V. Antisari, L. Giorgi, R. Marazzi, E. Piscopiello, A. Montone, S. Bellitto, S. Licoccia, E. Traversa, J. Power Sources 194 (2009) 243–251.
[44] R. Lamber, S. Wetjen, N.I. Jaeger, Phys. Rev. B: Solid State 51 (1995) 10968–10971.
[45] Y. Zhao, L. Zhan, J. Tian, S. Nie, Z. Ning, Electrochim. Acta 56 (2011) 1967–1972.
[46] B.D. Cullity, Elements of X-ray Diffraction, second ed., Addison-WesleyReading, 1956.
[47] K.H. Lee, S.W. Han, K.Y. Kwon, J.B. Park, J. Colloid Interface Sci. 403 (2013) 127–133.
[48] A. Jorio, R. Saito, G. Dresselhaus, M.S. Dresselhaus, Raman Spectroscopy in Graphene Related Systems, Wiley-VCH Verlag GmbH & Co. KGaA, Weinheim, 2011.
[49] J.I. Paredes, S. Villar-Rodil, P. Solís-Fernández, A. Martínez-Alonso, J.M.D. Tascón, Langmuir 25 (2009) 5957–5968.
[50] I.K. Moon, J. Lee, R.S. Ruoff, H. Lee, Nat. Commun. 1 (2010) 1–6.
[51] Y. Xu, H. Bai, G. Lu, C. Li, G. Shi, J. Am. Chem. Soc. 130 (2008) 5856–5857.
[52] S. Park, R.S. Ruoff, Nat. Nanotechnol. 4 (2009) 217–224.
[53] D.R. Dreyer, S. Park, C.W. Bielawski, R.S. Ruoff, Chem. Soc. Rev. 39 (2010) 228–240.
[54] O.C. Compton, S.B.T. Nguyen, Small 6 (2010) 711–723.
[55] Z.-X. Cai, C.-C. Liu, G.-H. Wu, X.-M. Chen, X. Chen, Electrochim. Acta 112 (2013) 756–762.
[56] F. Hasché, M. Oezaslan, P. Strasser, ChemCatChem 3 (2011) 1805–1813.
[57] F. Hasché, M. Oezaslan, P. Strasser, Phys. Chem. Chem. Phys. 12 (2010) 15251–15258.
[58] K. Kinoshita, J.T. Lundquist, P. Stonehart, J. Electroanal. Chem. Interfacial Electrochem. 48 (1973) 157–166.
[59] J. Durst, A. Lamibrac, F. Charlot, J. Dillet, L.F. Castanheira, G. Maranzana, L. Dubau, F. Maillard, M. Chatenet, O. Lottin, Appl. Catal. B 138–139 (2013) 416–426.
[60] P.S. Fernández, A. Arenillas, E.G. Calvo, J.A. Menéndez M.E. Martins, Int. J. Hydrog. Energy 37 (2012) 10249–10255.
[61] Y. Shao-Horn, W.C. Sheng, S. Chen, P.J. Ferreira, E.F. Holby, D. Morgan, Top. Catal. 46 (2007) 285–305.
[62] K.J.J. Mayhofer, S.J. Ashton, J.C. Meier, G.K.H. Wiberg, M. Hanzlik, M. Arenz, J. Power Sources 185 (2008) 734–739.

Cauê A. Martins received his B.S. degree (2008) in Chemistry, M.S. degree (2011) in Physical Chemistry and Ph.D. degree (2013) in Chemistry from the Institute of Chemistry at Federal University of Mato Grosso do Sul, Brazil. He developed part of his graduate research at Universidade Nacional de La Plata in Argentine and at Biodesign Institute from Arizona State University in United States. He currently holds a postdoctoral position at Federal University of Grande Dourados in Brazil. His current research involves development and evaluation of the electroactivity of nanocatalysts for fuel cells applications, mainly involving electrochemical and spectroelectrochemical techniques.

Pablo S. Fernández graduated in Chemistry at the University of La Plata (UNLP) in (2007) and received his Ph.D. at the same university in 2011. During 2012-2013 he worked at the INIFTA-UNPL as a postdoctoral researcher. He currently holds a postdoctoral position at the Institute of Chemistry of São Paulo-USP (Brazil). He has experience in Physical-Chemistry, and more specifically in the field of electrochemistry. His research projects focus on understanding the process occurring at electrified interfaces of noble metals and electrolytic solutions, especially in the presence of small organic molecules with energetic potential (ethanol, glycerol, etc.).

Fabio Lima graduated in Chemistry at the University of the State of Mato Grosso do Sul (2007) and received his Master's Degree in Chemistry from the Federal University of Mato Grosso do Sul (2010). Currently he is a Ph.D. student at the same university and has experience in electrochemistry and electroanalysis. His research is mainly focused on the oxygen reduction reaction (ORR), direct electronic transfer of enzymes. He is also interested in the synthesis of supports for fuel cell catalysts, as graphene, graphene oxide, and graphene nanoribbons.

Horacio E. Troiani is current and independent researcher at the Metals Physics Group at Centro Atómico Barilohe (CNEA), JTP at Instituto Balseiro, (UNCu) and CONICET (Argentina). His research interests comprehend nanoscience, carbon nanostructures, catalysis and fuel cells, metals and alloys, magnetic nanostructures, bio-remediation, transmission electron microscopy and related techniques. He has published 98 peer-reviewed papers, 6 books chapters and 1 patent, besides numerous posters, abstracts and presentations at international conferences. He also acts as a referee for international journals. He is the director of several postdoctoral fellows and 1 Ph.D. thesis. He participates of several evaluation committees at CONICET (Argentina).

María Elisa Martins graduated from National University of La Plata, receiving his Licentiate and Doctorate Degrees in Chemistry in 1965 and 1968, respectively. She is Titular Professor at UNLP (Electrochemistry and Surfaces). She joined CONICET in 1970 where she has been working since then, with stays in University of Paris, University of São Paulo and UFMS. She directed several Doctoral and Postdoctoral works. Nowadays, her research focuses on processes at electrified interfaces; noble metals; development of nanomaterials used as catalysts; electro-oxidation of alcohols. She leads various research projects on these fields and has co-authored 116 papers and book chapters.

Ana Arenillas graduated from University of Oviedo (Spain), where he received his M.Sc. in Chemistry and Ph.D. in Chemical Engineering in 1994 and 1999, respectively. She joined INCAR-CSIC (Spain) in 1995 where she has been working since then, with stays in Leeds University (UK) between 1995 and 1997 and Nottingham University (UK) between 2003 and 2004. Her research activity is mainly focused in carbon materials and their use in energy and environmental issues, besides the use of microwave heating applied to carbon-related technological processes. She leads various research projects on these fields. She is co-author of more than 100 papers, book chapters and patents.

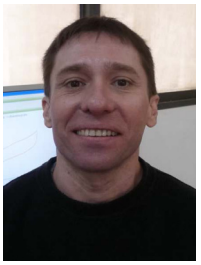

Gilberto Maia graduated in Chemistry at the Federal University of Ceará (1987), M. Sc. (1990) and Ph.D. (1994) in Physical Chemistry at the University of São Paulo-São Carlos. He has post-doctorate positions by the University of Liverpool, UK (2000) and Institute National Polytechnique de Grenoble, France (2011). He is currently Associate Professor at the Federal University of Mato Grosso do Sul and has published 31 articles in periodicals, acting mainly in electrochemistry, nanomaterials, oxygen reduction reaction, metallic nanostructured electrocatalysts, enzymatic bioelectrocatalysts, bacterial biofilms, films obtained from diazonium salts, graphene, graphene oxide, nanoribbons, DFT, electrocatalysts for alcohols and aldehydes.

Giuseppe A. Camara has received his Licenciate Degree in Chemistry from UERN (1997) and his M.S. in Physical Chemistry from UFRN (1999). In 2003 he received his Doctorate in Science from IQSC-USP and remained there for another three years with a post-doctorate position at the Electrochemistry Group. He is currently a Tenured Professor at the Institute of Chemistry of the Federal University of Mato Grosso do Sul (Brazil). His main research focuses on the development of nanomaterials aiming its application in renewable systems and on the study of the electrooxidation of alcohols candidate to be used in fuel cells.